

Synthesis of a Highly Selective Scavenger of Precious Metals from a Printed Circuit Board Based on Cellulose Filter Paper Functionalized with a Grafted Polymer Chain Bearing *N*-Methyl-2-hydroxyethylcarbamothioate Moieties

M. K. Mohammad Ziaul Hyder and Bungo Ochiai*



Cite This: *ACS Omega* 2022, 7, 10355–10364



Read Online

ACCESS |



Metrics & More

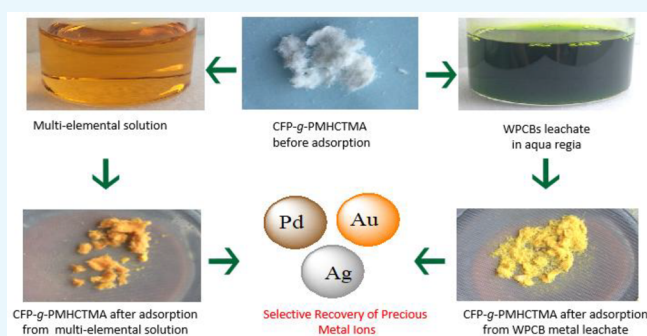


Article Recommendations



Supporting Information

ABSTRACT: We report the synthesis and practical application of a novel scavenger for precious metals. The scavenger was prepared from cellulose filter paper with grafted chains of poly(glycidyl methacrylate) modified with a novel ligand group of *N*-methyl-2-hydroxyethylcarbamothioate moieties, introduced by the reaction with *O*-1-mercapto-3-phenoxypropan-2-yl *N*-methyl-2-hydroxyethylcarbamothioate. Batch experiments were performed to evaluate the capability of the scavenger in ranges of pH and acid concentration as well as to determine the kinetics and isotherm models. The scavenger was found to adsorb only Ag(I), Pd(II), and Au(III) from an aqueous media in the presence of coexisting ions of different bases and precious metals at wide ranges of pH and acid concentration. The adsorption rates fit a pseudo-second-order kinetic equation, and the adsorption reached equilibrium within 60 min. The isotherm studies indicated that the obtained data were a good fit with the Langmuir model. The maximum adsorption capacities of Ag(I), Pd(II), and Au(III) were 126.95, 124.67, and 230.67 mg g⁻¹, respectively. Regeneration experiments indicated that the adsorbent maintained 97% of its initial efficiency even after five adsorption/desorption cycles. The scavenger was effectively utilized to recover Ag(I), Pd(II), and Au(III) from an aqua regia solution of waste printed circuit boards.



1. INTRODUCTION

Precious metals are widely used in diverse applications such as catalysis, electronics, automobiles, jewelry, and so on. In addition, the recent advance of technology is widening the field of their application more and more. However, the natural deposits and occurrences of the precious metals are limited. The recent technological advancements of electrical and electronic equipment are rapidly changing our lifestyles, resulting in a discharge of a substantial amount of waste electrical and electronic equipment at a quick pace.^{1–4} The quick production is accelerating the consumption of valuable metals such as gold, silver, and palladium. Consequently, waste electrical and electronic equipment is an essential resource for recovering valuable metals.^{5,6} Printed circuit boards are the key components of electrical and electronic equipment, where large amounts of valuable metals are used, and hence, these are considered as a greater source of precious metals than natural high-grade ores.^{7–10} Further, the amounts of these treasured metals are diminishing and in many mines are already exhausted. As a result, viable recuperation of these valuable metals from secondary assets such as waste printed circuit boards (WPCBs) is quite crucial from economic and

environmental points of view.^{11,12} The precious metals in circuit boards coexist with other base metals, and their ratios and the coexisting metals are widely different. The aqueous chemistry of metal ions sometimes differs whether they are in individual solutions or in mixtures with other metal ions. Hence, the recovery of precious metals from multielemental mixtures is quite difficult. Therefore, materials for the recovery of precious metals must have no affinity with other coexisting metal ions such as copper, iron, and zinc, which are abundantly used in electronics.¹³

The recovery of precious metals is carried out by various methods such as a hydrometallurgical process, membrane filtration, extraction, and ion exchange, but these processes are often accompanied by problems in selectivity, rate, cost, and difficulty of operation.^{14–17} Thus, it is crucial to develop

Received: December 10, 2021

Accepted: March 2, 2022

Published: March 14, 2022



economically practical and sufficiently selective methods and materials for the recovery of precious metals.¹⁸ Low-cost adsorbents with excellent selectivity toward the target precious metals are expected to provide a beneficial solution to this problem.

Modified cellulose materials have been attracting significant attention as efficient and cost-effective bio-based adsorbents.^{19–21} Cellulose is the most abundant biopolymer with outstanding physical and chemical properties. Cellulose can be easily modified by oxidation, etherification, esterification, and graft copolymerization due to the active hydroxyl groups of the cellulose at the 2-, 3-, and 6-positions.^{22–24} Various chemically functionalized celluloses have been designed for the efficient recovery of heavy metals^{25,26} and precious metals.^{19,22,27,28} Incorporating sulfur functional groups on polymers is a promising approach for the design of adsorbents for soft metals. Adsorption characters of adsorbents, such as selectivity and adsorption capacity, depend on the structures of the sulfur functional groups bound to the adsorbents.²⁹ While sulfur functional groups have affinities with soft metals, most sulfur functional groups, such as thiourea^{30,31} and dithiocarbamate anions,^{32–35} are not effective for selective attraction due to their affinities with wide ranges of metals. The selective collection of precious metals such as Ag(I), Pd(II), and Au(III) requires appropriate designs of the ligands.^{36–38} We have focused on soft thiocarbonyl moieties with a lower contribution of harder tautomeric thiol groups.^{29,39} For the support of the sulfur ligand, the authors have focused on cellulose filter paper (CFP) that is advantageous due to its abundance, inexpensiveness, accessibility, mechanical strength, and high surface area.^{40,41} In our previous work, we synthesized the effective adsorbent CFP-*g*-PHCTMA from *O*-1-mercapto-3-phenoxypropan-2-yl-2-hydroxyethylcarbamothioate (HCT) and CFP grafted with poly(glycidyl methacrylate) (CFP-*g*-PGMA). CFP-*g*-PHCTMA showed good and selective adsorption capability toward the precious metals Ag(I), Pd(II), and Au(III).⁴² The adsorption reached equilibrium within 60 min for both Au(III) and Pd(II), whereas it reached equilibrium at a slower rate for Ag(I) of 120 min. The Langmuir monolayer adsorption capacities of the Ag(I), Pd(II), and Au(III) ion species were found to be 78.26, 92.35, and 152.38 mg g⁻¹, respectively.

Encouraged by this result, we designed the novel adsorbent CFP-*g*-PMHCTMA bearing the novel selective ligand *N*-methyl-2-hydroxyethylcarbamothioate by the reaction of CFP-*g*-PGMA and *O*-1-mercapto-3-phenoxypropan-2-yl *N*-methyl-2-hydroxyethylcarbamothioate (MHCT). We synthesized the MHCT ligand, the *N*-methyl analogue of the HCT ligand,⁴² for systematic studies of the adsorption properties of precious-metal ions. The adsorption manners of CFP-*g*-PMHCTMA toward precious metals were investigated on the basis of selectivity, adsorption isotherm, and kinetics for a better understanding of the mechanism of adsorption of precious metals. The empirical recuperation of Ag(I), Pd(II), and Au(III) from WPCB leachate in aqua regia utilizing CFP-*g*-PMHCTMA was also demonstrated in this study.

2. SYNTHESIS AND CHARACTERIZATION OF THE NOVEL LIGAND

2.1. Synthesis of MHCT. MHCT was prepared by the previously reported method for HCT.⁴² DTC (2.26 g, 10.0 mmol) and *N*-methylaminoethanol (9.01 g, 12.0 mmol) was stirred for 3 h in THF (5 mL) at room temperature under an

N₂ atmosphere. Volatile substances were removed under reduced pressure. MHCT was obtained by silica gel column chromatography with CHCl₃/MeOH as eluent (v/v = 1/0.05). Yield: 2.03 g, 6.75 mmol, 67.5%. The product was analyzed only by ¹H and ¹³C NMR spectroscopy due to the low stability of the thiol group.

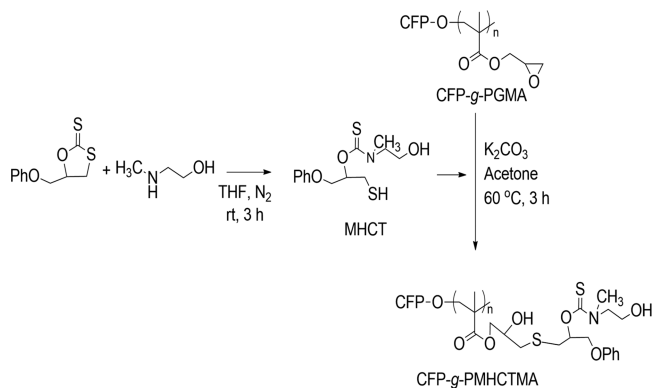
¹H NMR (400 MHz, CDCl₃): 2.99 (–CH₂SH), 3.07–3.44 (*cis*- or *trans*-NCH₃), 3.59–3.69 (–CH₂CH₂OH), 3.84–3.92 (–CH₂OH), 4.25–4.28 (C₆H₅OCH₂–) 5.72–5.78 (–CH₂CHOCH₂–), 6.92 (C₆H₅–), 7.25 (–C₆H₅) ppm (Figure S1).

¹³C NMR (100 MHz, CDCl₃): 24.73 (–CH₂SH), 37.61 and 42.47 (*cis* or *trans*-NCH₃–), 53.13 and 56.82 (–CH₂CH₂OH), 60.62 and 60.99 (C₆H₅OCH₂–), 66.43 (–CH₂OH), 79.35 and 79.72 (–CH₂CHOCH₂–), 114.79, 121.49, 129.63, 158.34 (–C₆H₅), 188.56 (–OC=S) ppm (Figures S2 and S3).

2.2. Acylation of MHCT. MHCT was acetylated to protect the –OH and –SH groups for further cyclization of the structure of MHCT. DTC (0.226 g, 1.00 mmol) and *N*-methylaminoethanol (0.090 g, 1.2 mmol) were reacted in THF (5 mL) for 3 h at room temperature under an N₂ atmosphere. Then, acetic anhydride (1.0 g, 10 mmol) and triethylamine (0.020 g, 2.0 mmol) were added to the reaction mixture, and the reaction was allowed to continue for 18 h. The acetylated product was obtained just by washing once with a brine solution and twice with distilled water and characterized by ¹H NMR (400 MHz, CDCl₃) (Figure S4) and ¹³C NMR (100 MHz, CDCl₃) (Figure S5).

2.3. Synthesis of the Novel Scavenger CFP-*g*-PMHCTMA. CFP-*g*-PMHCTMA was synthesized as shown in Scheme 1 by following the previously reported method for

Scheme 1. Synthesis of MHCT and CFP-*g*-PMHCTMA



CFP-*g*-PHCTMA, the NH analogue of CFP-*g*-PMHCTMA.⁴² CFP-*g*-PGMA (1.0 g) was added to a mixture of MHCT (2.0 equiv with respect to the GMA unit) and K₂CO₃ (2.0 equiv with respect to the GMA unit) in 10 mL of acetone, and the mixture was stirred at 60 °C for 3 h under a nitrogen atmosphere. CFP-*g*-PMHCTMA was consecutively washed with water, methanol, and acetone and was dried at 60 °C under vacuum for 24 h.

3. RESULT AND DISCUSSION

3.1. Synthesis and Characterization of CFP-*g*-PMHCTMA. The *N*-methylthiourethane skeleton in CFP-*g*-PMHCTMA was fabricated by the reaction of *N*-methylaminoethanol and a cyclic dithiocarbonate. The *N*-methyl mercaptothiourethane was used for modification of CFP-*g*-

PGMA by the nucleophilic ring-opening addition of the thiol moieties to the epoxy rings under basic conditions.

CFP-g-PMHCTMA was characterized by FTIR and EDX spectroscopic analyses. The FTIR spectra of CFP, CFP-g-PGMA, and CFP-g-PMHCTMA are represented in Figure 1.

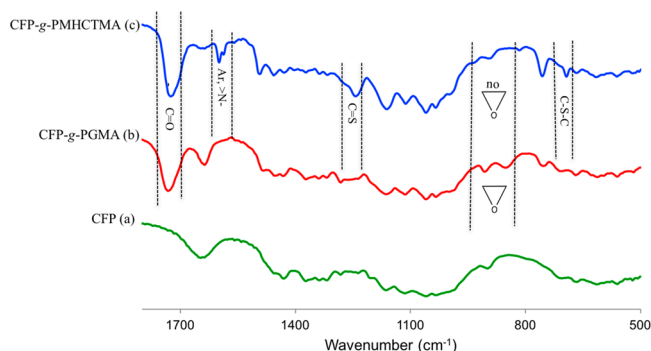


Figure 1. FTIR spectra of (a) CFP, (b) CFP-g-PGMA, and (c) CFP-g-PMHCTMA.

The characteristic absorption band of the carbonyl moieties at 1728 cm^{-1} and those of the epoxy moieties at 849 and 907 cm^{-1} appeared in the FTIR spectrum of CFP-g-PGMA (Figure 1b), which was not found in the spectrum of CFP (Figure 1a). The characteristic peaks of the C=S moieties, the NH moieties, and the aromatic ring of the MHCT ligand at 1243 , 1587 , and 1598 cm^{-1} , respectively, were observed in the FTIR spectrum of CFP-g-PMHCTMA (Figure 1c), which were not observable in the spectrum of CFP-g-PGMA or in the spectrum of CFP. Moreover, the absorptions of the epoxy moieties observed at 849 and 907 cm^{-1} for CFP-g-PGMA are not observable in the spectrum of CFP-g-PMHCTMA, strongly indicating the effective incorporation of the MHCT ligand. The introduction of the sulfur-containing structure was further confirmed by the EDX spectrum of CFP-g-PMHCTMA (Figure S6c) showing a characteristic peak of sulfur at 2.3 keV in addition to the original carbon and oxygen peaks observed in the EDX spectra of CFP-g-PGMA (Figure S6b) and CFP (Figure S6a).

3.2. Adsorption Behavior of CFP-g-PMHCTMA toward Various Metal Ions. The adsorption behaviors of CFP-g-PMHCTMA toward various metal ions—namely Cu(II), Ag(I), Ni(II), Os(IV), Pd(II), Pt(IV), Au(III), Re(VII), and Rh(III)—from their individual solutions were investigated to understand the selectivity of the adsorbent (Figure 2). CFP-g-PMHCTMA was highly selective toward Ag(I), Pd(II), and Au(III) with an excellent adsorption capacity exceeding that of CFP-g-PHCTMA and showed very weak affinity with Cu(II) and Pt(IV) metal ions. Other precious and base metals were not adsorbed at all, similarly to the case for CFP-g-PHCTMA. This selective adsorption ability of CFP-g-PHCTMA agrees with Pearson's hard–soft acid–base concept,⁴⁴ where the very soft Lewis basicity of the thione functional groups on CFP-g-PMHCTMA results in high affinity with the very soft Lewis acids Ag(I), Pd(II), and Au(III). Losev et al.⁴⁵ reported that an adsorbent bearing dialkylthiourea moieties adsorbs Ag(I), Pd(II), Au(III), and Pt(IV) due to their labile properties and has negligible affinity toward Rh(III), Ru(IV), Ir(IV), and Os(IV) due to their harder characteristics and that an adsorbent bearing disulfide moieties shows higher selectivity. Hence, the higher selectivity of the MHCT ligand toward Ag(I), Pd(II), and Au(III) can be attributed to the absence of the contribution of the iminothiol tautomeric structure with harder basicity.

The adsorbents after the adsorption of Ag(I), Pd(II), and Au(III) were analyzed by EDX. The clear peaks of Ag(I), Pd(II), and Au(III) that appeared in the EDX spectra indicate the adsorption of these metal ions onto CFP-g-PMHCTMA (Figure S7).

3.3. Effect of pH on Adsorption of Ag(I), Pd(II), and Au(III) Ions. The effect of pH on the adsorption of metal ions on CFP-g-PMHCTMA was studied over the range of $1.20 \leq \text{pH} \leq 5.95$, and the results are presented in Figure 3a. The experiments at varying pH were conducted with 5 mL amounts of 200 mg L^{-1} aqueous solutions of Ag(I) and Pd(II) and 300 mg L^{-1} aqueous solutions of Au(III) on contact with 5 mg of CFP-g-PMHCTMA. The pH was adjusted with aqueous solutions of HCl and NaOH. The suspensions were agitated with a mechanical shaker for 24 h at $25\text{ }^{\circ}\text{C}$. The uptakes of Au(III) and Ag(I) remained almost constant from pH 1.20 to

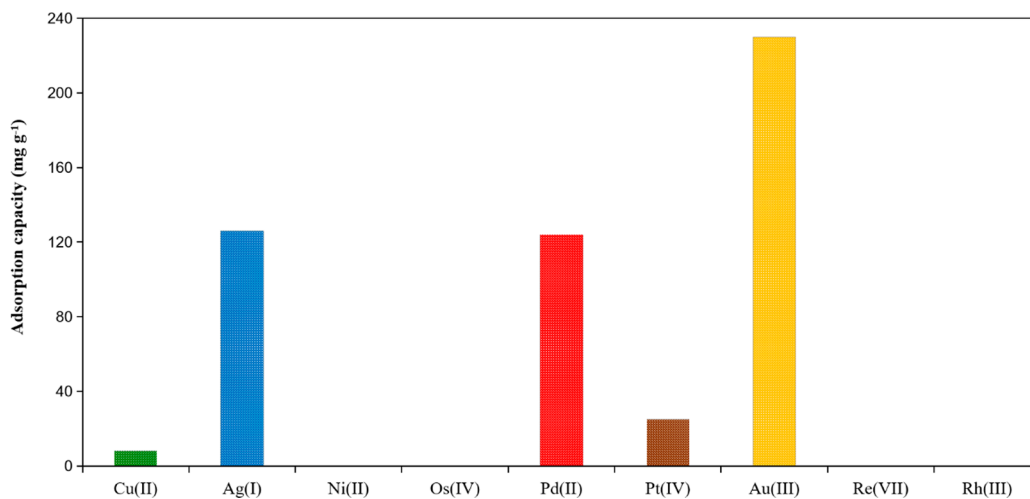


Figure 2. Adsorption of single metal ions from individual solutions of Cu(II), Ag(I), Ni(II), Os(IV), Pd(II), Pt(IV), Au(III), Re(VII), and Rh(III) by CFP-g-PMHCTMA. Conditions: concentrations of Cu(II), Ag(I), Ni(II), Os(IV), Pd(II), Pt(IV), Re(VII), and Rh(III), 200 mg L^{-1} ; concentration of Au(III), 280 mg L^{-1} ; CFP-g-PMHCTMA, 1 g L^{-1} ; pH 3.1 ; $25\text{ }^{\circ}\text{C}$; 24 h .

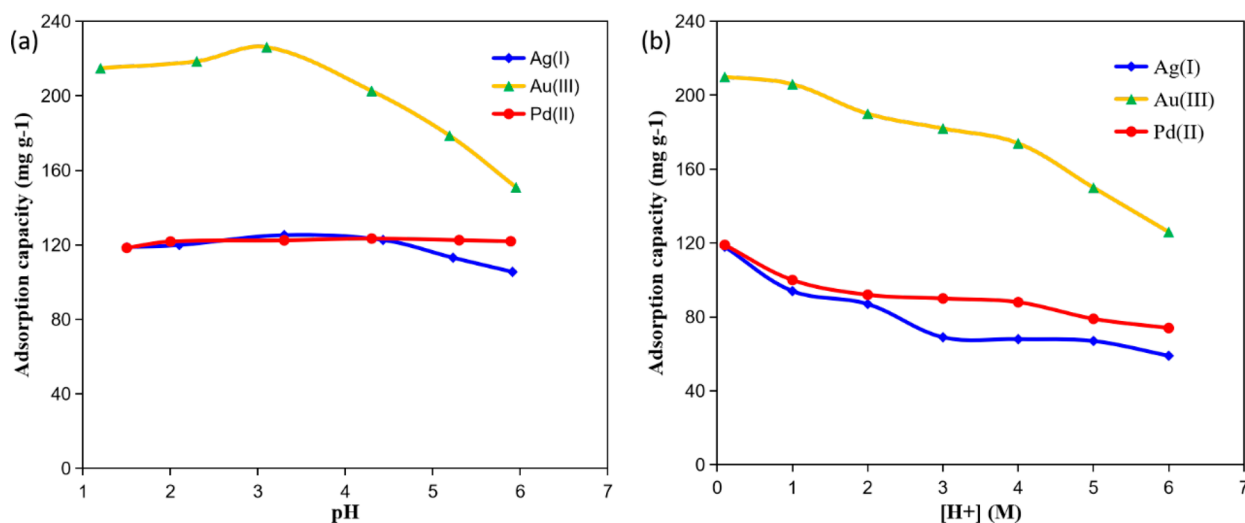


Figure 3. (a) Effect of pH on the adsorption of Ag(I), Pd(II), and Au(III) ions. (b) Effect of [H⁺] concentration on the adsorption of Ag(I), Pd(II), and Au(III) onto CFP-g-PMHCTMA. Conditions; initial concentration of Ag(I) and Pd(II), 200 mg L⁻¹, initial concentration of Au(III), 300 mg L⁻¹, CFP-g-PMHCTMA, 1 g L⁻¹; 24 h; 25 °C.

3.10 and pH 1.20 to 4.43, respectively, and dropped at the higher pH region. In contrast, the uptakes of Pd(II) were almost identical in the examined range of pH. The adsorption capacity became the highest for Ag(I), Pd(II), and Au(III) at pH 3.1, pH 4.30, and pH 4.43, respectively. Earlier studies on the uptake of these precious metals indicated the suitable pH was from 1.0 to 4.0.^{46,47} The constant uptake of the metal ions over the wide range of pH probably originates from the negligible competition of hard H⁺ toward the target precious metals on interaction with the soft thiocarbamate ligand even under highly acidic conditions. The most plausible structure of the complexes is based on the coordination of the free lone pair electron of the sulfur atom to the metal ions. The decrease in uptakes observed for Ag(I) and Au(III) at pHs higher than 4.0 probably originated from the hydrolysis of the metal ions to form hydroxide complexes.^{48,49}

3.4. Effect of H⁺ Ion Concentration on Adsorption Procedure. This is an important requirement for metal scavengers for the selective adsorption of precious metals in strong acid with a view to determining empirical hydro-metallurgical collections of precious metals, as leaching of a metal is often carried out with concentrated acids. Hence, adsorption isotherm studies under highly acidic conditions were carried out for Pd(II) and Au(III) in aqueous HCl and for Ag(I) in aqueous HNO₃ (Figure 3b). Quantitative amounts of Ag(I), Pd(II), and Au(III) were adsorbed by CFP-g-PMHCTMA even at 6 M acid concentration. The outstanding adsorption capacity of CFP-g-PMHCTMA at a higher acid concentration places this adsorbent as a viable candidate for the empirical recovery of Ag(I), Pd(II), and Au(III) from waste streams.

The adsorption capacity for Ag(I), Pd(II), and Au(III) decreased upon an increase in the acid concentration, while the capacity is higher than that of CFP-g-PHCTMA⁴² even at a higher acid concentration. The reduced adsorption capacities at higher acid concentrations can be illustrated by the marginal protonation of sulfur atoms in the thione functional groups of CFP-g-PMHCTMA under the very acidic conditions (Figure 4), as described in the adsorption of Au(III) and Pd(II) by phosphine sulfide type chelating polymers⁵⁰ and by the

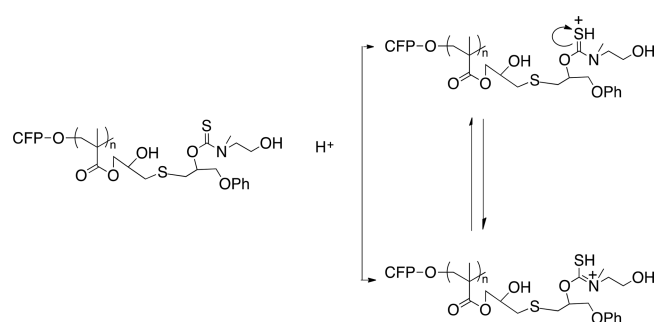


Figure 4. Scheme of the protonation of the sulfur atom on functional groups.

competition between protons and Ag(I), Pd(II), and Au(III) for the adsorption positions on the CFP-g-PMHCTMA.²¹

3.5. Adsorption Isotherm. Adsorption isotherms provide important information on adsorption mechanisms in the design of sorption systems. Figure 5 represents the isotherms for batch adsorption of Ag(I), Pd(II), and Au(III) by CFP-g-PMHCTMA at pH 3.0. The weight-based adsorption isotherms shown in Figure 5a confirm that the uptake capacities for Ag(I), Pd(II), and Au(III) at the equilibria increase with an increase in the concentration of the metal solutions. An adsorption capacity exceeding 100 mg g⁻¹ is high among selective adsorbents. Typical adsorbents with capacities above 100 mg g⁻¹ employ weakly selective adsorption groups such as ethylenediamine and amino acid or contain non-specifically binding substrates such as chitosan and graphene oxide.⁵¹ The high capacity along with the selectivity described below is the significant advantage of CFP-g-PMHCTMA. The improved adsorption capacities probably originated from the excellent affinity of the *N*-methylthiocarbamothioate ligand. For a better explanation of the relationship between the adsorption capacity and the equilibrium concentration of the metal ions, the Langmuir isotherm (eq 1) (Figure 5b) and Freundlich isotherm (eq 2) were investigated by fitting the experimental data for the batch adsorption isotherm

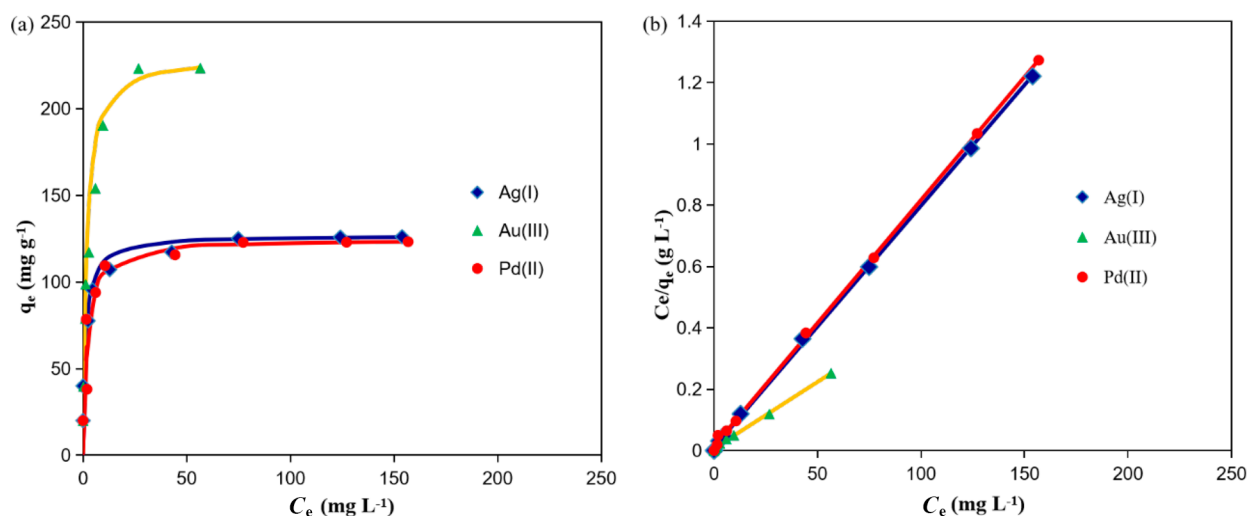


Figure 5. Isotherm of (a) adsorption capacity of Ag(I), Pd(II), and Au(III) ions in milligrams. (b) Linear plots of the Langmuir isotherms of adsorption of Ag(I), Pd(II), and Au(III) on CFP-g-PMHCTMA. Conditions: initial concentration of Ag(I), Pd(II), and Au(III) ions, 20–300 mg L⁻¹; CFP-g-PMHCTMA, 1 g L⁻¹; pH 3.0; 25 °C; 24 h.

$$\frac{C_e}{q_e} = \frac{1}{K_L q_m} + \frac{C_e}{q_m} \quad (1)$$

$$\ln q_e = \ln K_f + \frac{1}{n} (\ln C_e) \quad (2)$$

where q_e (mg g⁻¹) is the amount of metal ion adsorbed at equilibrium, q_m (mg g⁻¹) is the maximum adsorption in a monolayered adsorption system, C_e (mg L⁻¹) is the equilibrium concentration of metal ions in solution, K_L (L g⁻¹) is the Langmuir adsorption equilibrium constant related to adsorption energy, K_F (L g⁻¹) is the Freundlich adsorption equilibrium constant related to adsorption capacity, and n is an empirical parameter related to the adsorption intensity.

The Langmuir adsorption isotherm model was presumably utilized on the basis of adsorbing one metal ion by each C=S moiety. The adsorbed quantities of Ag(I), Pd(II), and Au(III) ions at the equilibria (q_e) was found to increase with an increase in the initial metal ion concentrations, and plateau regions were noted at high concentrations of the metal ions. This implies the monolayer adsorption of this adsorption system, which corresponds to Langmuir-type adsorption.⁵² Moreover, the linear correlation between the metal ion concentration at equilibrium (C_e) and C_e/q_e reveals that the experimental data have a better fit to the Langmuir isotherm model in comparison to the Freundlich isotherm model (Table S1 and eqs 1 and 2) in the same manner as that for the S-modified cellulose adsorbent previously reported⁴² and similar to those of other S-modified celluloses,^{53,54} indicating that the active adsorption sites contributed equally to the adsorption process. The adsorbed amounts of Ag(I), Pd(II), and Au(III) calculated from the Langmuir isotherm studies were determined to be 126.95, 124.67, and 230.67 mg g⁻¹, respectively. These figures are near the molar amount of C=S in CFP-g-PMHCTMA (1.32 mmol g⁻¹) and the almost equimolar adsorption of Ag(I) (1.17 mmol g⁻¹), Pd(II) (1.19 mmol g⁻¹), and Au(III) (1.17 mmol g⁻¹) on CFP-g-PMHCTMA, indicating that most of the adsorption sites on the adsorbent are active. The total results denote the complexation between the metal ions and the thiocarbamate

moieties in a 1:1 stoichiometry in the adsorbent with excellent efficiency.

Furthermore, these capacities are significantly higher than those of the previously reported CFP-g-PHCTMA,⁴² for which the adsorption capacities toward Ag(I), Pd(II), and Au(III) were 78.26, 92.35, and 152.38 mg g⁻¹, respectively. The higher adsorption capacity of CFP-g-PMHCTMA toward Ag(I), Pd(II), and Au(III) is ascribed to the incorporation of a greater amount of C=S contents. The introduction ratio of the ligand structure in CFP-g-PMHCTMA being higher than that of CFP-g-PHCTMA probably originates from the absence of the thiourea proton with a higher acidity in comparison to the thiol group, which was included in the previous ligand. This functionalization proceeds through the nucleophilic addition of thiolate moieties produced by a hydrogen abstraction with triethylamine, and the presence of active protons with acidities higher than that of the thiol group delays the reaction. The higher acidity of the thiourea proton can be confirmed by its ¹H NMR signal appearing at 6.95 ppm, being at a lower magnetic field in comparison to the signal of the thiol proton appearing at 2.98 ppm.⁴²

As is evident from this isotherm study, the adsorption proceeded on the homogeneous C=S sites binding metal ions in the 1:1 stoichiometry. A plausible structure of the binding site in CFP-g-PMHCTMA is illustrated in Figure 6. The most important binding site is the C=S moieties, but the sulfide moieties might assist the ligation.

3.6. Effect of Contact Time and Studies of Adsorption Kinetics.

Fast uptake of precious metals is an important

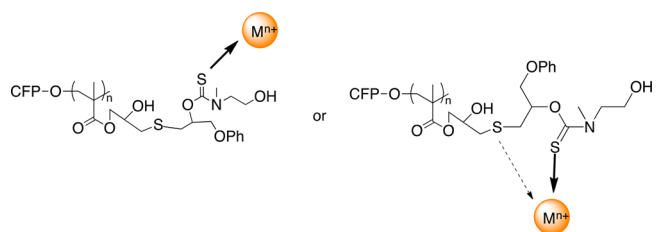


Figure 6. Plausible mechanism of adsorption of metal ions on the functional groups of CFP-g-PMHCTMA.

feature of scavengers for precious metals from waste streams. To confirm the rates of the adsorption, adsorption experiments were carried out for 10 mg L⁻¹ of Ag(I), Pd(II), and Au(III) solution using 1 g L⁻¹ adsorbent (Figure 7). The uptake exceeded 90% within 30 min, and the adsorption reached equilibrium within 60 min.

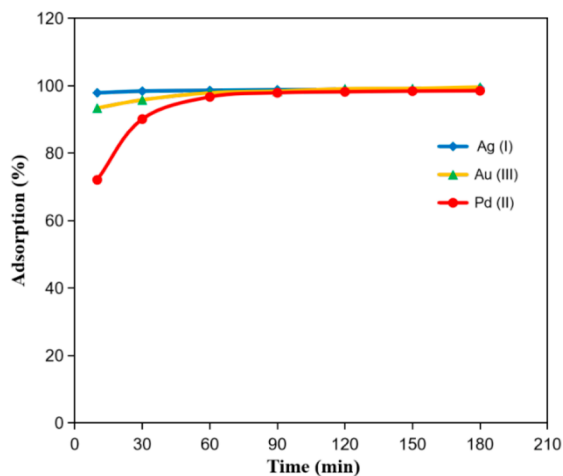


Figure 7. Effect of contact time of adsorption of Ag(I), Pd(II), Au(III) onto CFP-g-PMHCTMA. Conditions: initial concentration of each Ag(I), Pd(II), and Au(III) ions, 10 mg L⁻¹; CFP-g-PMHCTMA, 1 g L⁻¹; pH 3.1; 25 °C.

The adsorption rates of Ag(I), Pd(II), and Au(III) on CFP-g-PMHCTMA were measured at 25 °C to understand the kinetic mechanism of the adsorption process. The kinetics of adsorption was investigated with a pseudo-first-order kinetic model (eq 3) and its linear form (eq 4) and with a pseudo-second-order model (eq 5) and its linear form (eq 6).

$$q_t = q_e(1 - e^{-k_1 t}) \quad (3)$$

$$\ln(q_e - q_t) = \ln q_e - k_1 t \quad (4)$$

$$q_t = \frac{k_2 q_e^2 t}{1 + k_2 q_e t} \quad (5)$$

$$\frac{t}{q_t} = \frac{1}{k_2 q_e^2} + \frac{t}{q_e} \quad (6)$$

where q_e (mg g⁻¹) and q_t (mg g⁻¹) are the mass of adsorbed metal ions per unit mass of the adsorbent at equilibria and time (t), respectively, and k_1 (g mg⁻¹ min⁻¹) and k_2 (dm⁻³ mg⁻¹ min⁻¹) are the rate constants of pseudo-first-order and pseudo-second-order models, respectively. The kinetic results of adsorption were obtained by evaluating Figure 8.

The linearity in the pseudo-second-order plots (Figure 9a) is better than that of pseudo-first-order plots (Figure 9b), as proved by the higher R^2 values exceeding 0.997 (Table S2). This pseudo-second-order kinetics indicates that the rate-determining step of this adsorption is the chemical reaction between the metal ions and the adsorbent.

3.7. Selective Adsorption of Ag(I), Pd(II), and Au(III) from Multielemental Solutions. The recovery of precious metal ions has been conducted for multielemental solutions comprising a range of base metals such as nickel, copper, and zinc at high acid concentrations. In order to confirm the

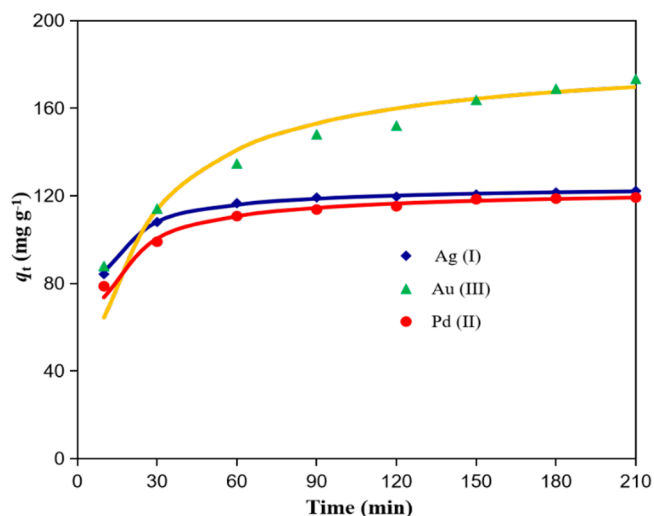


Figure 8. Adsorption kinetics of Ag(I), Pd(II), and Au(III) on CFP-g-PMHCTMA. Conditions: initial concentrations of Ag(I), Pd(II), and Au(III) ions, 200 mg L⁻¹; CFP-g-PMHCTMA, 1 g L⁻¹; pH 3.0–3.3; 25 °C.

selective adsorption ability of CFP-g-PMHCTMA toward precious-metal ions, adsorption experiments were performed using two types of multielemental solutions with various acid concentrations (Figure S8). Figure S8a represents the selective capture of Ag(I) from a multielemental solution (1) comprising Cu(II), Ag(I), Zn(II), Ni(II), Cd(II), V(V), Cr(III), Mn(II), Fe(III), and Co(III) in aqueous HNO₃ in an acid concentration range from 1 to 6 M. This result shows that CFP-g-PMHCTMA captures only Ag(I) from the mixture of different base-metal ions without coadsorption of other metals in the highly acidic media. Figure S8b shows the metal adsorption of CFP-g-PMHCTMA from a multielemental solution (2) comprising Ru(III), Rh(III), Au(III), Ir(III), Pd(II), Pt(IV), and Os(IV) in aqueous HCl in an acid concentration range from 1 to 6 M. Pd(II) and Au(III) were predominantly bound to the adsorbent. No other precious metals were adsorbed at all by CFP-g-PMHCTMA at higher acid concentrations, whereas very trace amounts of Pt(IV) and Os(IV) were found to be adsorbed at lower acid concentrations. These data indicate that specific precious metals can be selectively recovered from a mixture of various precious-metal ions even in highly acidic media. A possible factor for the trace adsorption of Os(IV) and no affinity toward Cu(II) from multielemental solutions by CFP-g-PMHCTMA is the effect of coexisting ions. Adsorption behaviors in multielemental solutions are often affected by the coexisting ions, and an analysis of the effects is very difficult due to the complexity, as reviewed by Neris et al.⁵⁵

CFP-g-PMHCTMA was employed for the study of adsorption from a mixture of 1 in HNO₃ media and 2 in HCl media (total acid concentration 1.53 M) (Figure S9). CFP-g-PMHCTMA was found to adsorb Ag(I), Pd(II), and Au(III) selectively and efficiently even from a mixture of the two multielemental solutions as well as the individual and the original multimetal solutions. The photo images of the state of CFP-g-PMHCTMA before and after adsorption from the mixtures of 1 and 2 are shown in Figure S10, indicating the coloring of the adsorbent after the adsorption.

3.8. Selective Recovery of Ag(I), Pd(II), and Au(III) from a WPCB Leachate. The metal adsorption behavior of

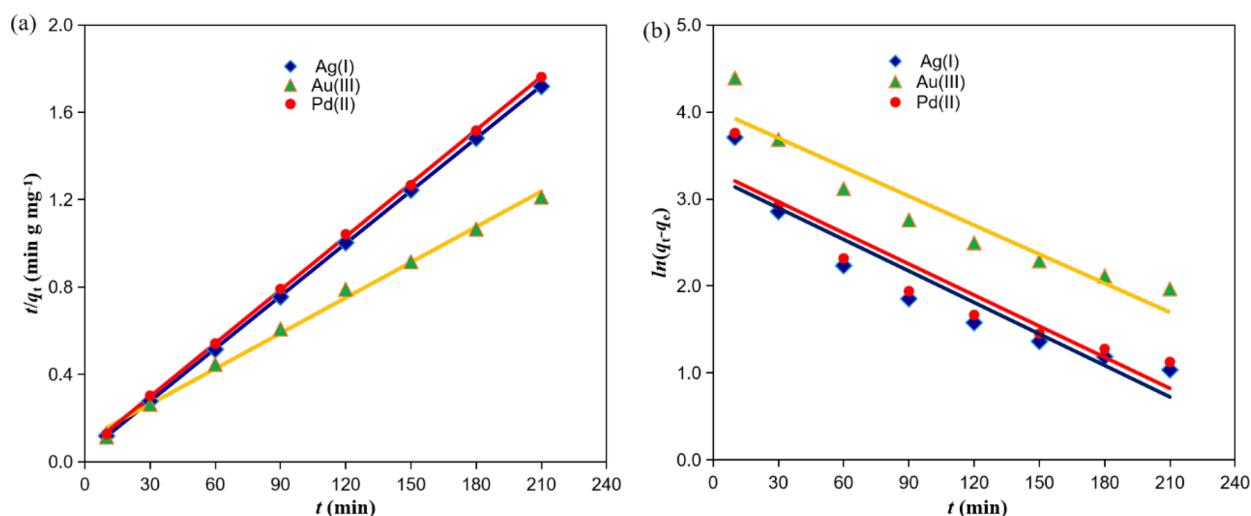


Figure 9. Linear plots of (a) pseudo-second-order kinetics and (b) pseudo-first-order kinetics of adsorption of Ag(I), Pd(II), and Au(III) ions on CFP-g-PMHCTMA. Conditions: initial concentrations of Ag(I), Pd(II), and Au(III) ions, 200 mg L⁻¹; CFP-g-PMHCTMA, 1 g L⁻¹; pH 3.0–3.3; 25 °C.

CFP-g-PMHCTMA from a WPCB metal leachate in aqua regia (Figure S11) was investigated, and the result is shown in Figure S12. Pd(II) and Au(III) were absolutely captured onto the adsorbent CFP-g-PMHCTMA, while Cu(II), Ni(II), V(V), Zn(II), and Fe(II) were negligibly captured. The adsorption capacity of Ag(I) was to be found lower than that of Au(III) and Pd(II), probably due to the formation of a stable complex in aqua regia.⁵⁶ Figure S13 shows that the color of CFP-g-PMHCTMA changed from white to yellow in a similar fashion with an adsorption from the mixture of the multielemental solutions shown in Figure S10. These results evidently demonstrate that the precious metals Ag(I), Pd(II), and Au(III) were effectively retrieved by CFP-g-PMHCTMA from the metal leachate from WPCBs containing a significantly higher concentration of various metals and unidentified compounds originating from WPCBs. Specifically, CFP-g-PMHCTMA is a potential and promising candidate for the practical recovery of precious metals.

3.9. Desorption of Precious Metals from Metal-Loaded CFP-g-PMHCTMA and Its Reuse Ability. The regeneration and reusability of an adsorbent is a vital feature from a consideration of practical and economical purposes. The desorption efficiency of the adsorbed precious metal (50 mg L⁻¹) onto 1 g L⁻¹ CFP-g-PMHCTMA was determined using various concentrations of HNO₃, thiourea-HNO₃, and thiourea solutions. The effect of the eluent on the desorption of the precious metals and the adsorption capacity of the regenerated adsorbent are presented in Table 1. HNO₃ solutions were not effective for desorption, as the degrees of desorption are less than 10% regardless of the concentrations. The 0.5 M thiourea solution performed better, while it was not effective enough. In contrast, quantitative desorption was attained using the eluent 0.1 M HNO₃ and 0.5 M thiourea, while lower concentrations of thiourea resulted in lower desorption efficiencies. The adsorbent after the desorption can be recycled. Table 2 shows the adsorption capacity during the five repeated adsorption–desorption processes relative to the initial capacity. The relative adsorption capacity exceeded 97% even at the fifth cycle, indicating the excellent durability of CFP-g-PMHCTMA.

Table 1. Desorption of Ag(I), Pd(II), and Au(III) from CFP-g-PMHCTMA after Adsorption of Metal Ions with Different Concentrations of HNO₃, Thiourea, and Their Mixtures^a

eluent	degree of desorption of metals (%)		
	Ag(I)	Pd(II)	Au(III)
0.5 M HNO ₃	0.3	1.5	0.6
1 M HNO ₃	0.4	4.4	0.9
2 M HNO ₃	0.8	10.6	1.0
0.1 M HNO ₃ + 0.1 M thiourea	61.9	53.2	76.0
0.1 M HNO ₃ + 0.3 M thiourea	83.2	75.9	100.0
0.1 M HNO ₃ + 0.5 M Thiourea	100.0	99.1	100.0
0.5 M thiourea	40.8	49.7	65.0

^aConditions: Ag(I), Pd(II), and Au(III), 50 mg L⁻¹; CFP-g-PMHCTMA, 1 g L⁻¹; 25 °C; desorption time, 3 h.

Table 2. Repeated Adsorption of Ag(I), Pd(II), and Au(III) Ions by CFP-g-PMHCTMA^a

cycle no.	relative adsorption capacity (%)		
	Ag(I)	Pd(II)	Au(III)
1	100.0	100.0	100.0
2	100.0	99.4	100.0
3	99.7	97.6	99.1
4	98.8	97.3	99.1
5	98.6	96.7	98.7

^aConditions: Ag(I), Pd(II), and Au(III), 50 mg L⁻¹; CFP-g-PMHCTMA, 1 g L⁻¹; 25 °C; contact time for each adsorption–desorption cycle, 3 h.

4. CONCLUSIONS

This study has shown that CFP-g-PMHCTMA is a promising adsorbent for the precious metals Ag(I), Pd(II), and Au(III) from the solutions containing various kinds of metals under a wide range of pH conditions, including high acid concentrations. CFP-g-PMHCTMA demonstrated an outstanding selectivity of adsorption toward Ag(I), Pd(II), and Au(III) from multielemental solutions containing various base and noble metals. These precious metals were selectively adsorbed with negligible adsorption of coexisting metal ions present in

excess. The efficiency of CFP-g-PMHCTMA relies on the *N*-methyl-2-hydroxyethylcarbamothioate ligand designed to make the Lewis basicity of the sulfur ligand softer by eliminating the contribution of the harder iminothiol tautomer. The adsorption capacity is higher than that of the $-NH$ analogue previously reported, probably due to the absence of active hydrogens competitively abstracted during the nucleophilic modification of the epoxy ring. The experimental data exactly fitted the Langmuir isotherm model and pseudo-second-order kinetics. The loaded metals from CFP-g-PMHCTMA can be effectively desorbed by 0.5 M thiourea in 0.1 M HNO_3 . CFP-g-PMHCTMA retained its original efficacy even after five times of reuse. CFP-g-PMHCTMA was shown to be an excellent scavenger for the selective recovery of Au(III), Pd(II), and Ag(I) from WPCB leachates in aqua regia. This investigation establishes that this cellulose-based CFP-g-PMHCTMA is an eco-friendly and economically viable selective adsorbent for precious metals due to its recyclability and high selectivity even in the presence of multiple ions.

5. EXPERIMENTAL SECTION

5.1. Chemicals. All the chemicals used were of analytical reagent grade. CFP (AdvantecSC; Toyo Roshi, Tokyo, Japan) was used for modification. Glycidyl methacrylate (GMA), potassium carbonate, sodium hydroxide, HCl, and *N*-methyl-2-aminoethanol were purchased from Kanto Chemical (Tokyo, Japan). $K_2H_2PO_4$ -NaOH-7.2 buffer solution was purchased from Tokyo Chemical Industry (Tokyo, Japan). Diammonium ceric(IV) nitrate (CAN), nitric acid, and Cu(II) ($Cu(NO_3)_2$) and Ni(II) ($Ni(NO_3)_2$) standards for ICP (1000 $mg\ L^{-1}$) were purchased from Wako Chemicals (Tokyo, Japan). Pd(II) ($Pd(NO_3)_2 + HCl$), Au(III) ($HAuCl_4$), Ag(I) ($AgNO_3$), Rh(III) ($HRhCl_4$), and Pt(IV) (H_2PtCl_6) standards for ICP (1000 $mg\ L^{-1}$), transition metal mix 1 (Cu(II), V(V), Ni(II), Co(II), Fe(III), Mn(II), Cr(III), Ag(I), Zn(II) and Cd(II)), and transition metal mix 2 (Pd(II), Au(III), Pt(IV), Ru(III), Rd(III), Os(IV), and Ir(III)) for ICP (100 mg/L) were purchased from Sigma-Aldrich (St. Louis, Missouri, USA). Re(VII) (NH_4ReO_4 in H_2O) and Os(IV) ($(NH_4)_2OsCl_6$ in 7% HCl) were purchased from Merck (Darmstadt, Germany). Water was purified with a MINIPURE TW-300RU apparatus (Nomura Micro Science, Kanagawa, Japan). 4-(Phenoxyethyl)-1,3-oxathiolane-2-thione (DTC) was prepared according to the literature.⁴³ CFP-g-PGMA with a grafting percentage of 156% was prepared as described in a previous work.⁴² In brief, grafting from the polymerization of GMA (1.20 g, 8.57 mmol) was carried out with CFP (0.60 g) in 20 mL of water for 30 min in the presence of a freshly prepared 0.005 M solution of CAN in 10 mL of 0.1 M HNO_3 .

5.2. Measurements. 1H and ^{13}C NMR spectra were recorded on a JEOL ECX 400 NMR spectrometer (400 MHz for 1H and 100 MHz for ^{13}C). FTIR spectra were recorded on a JASCO FT/IR-460 plus Fourier transform infrared spectrophotometer in a KBr matrix. Energy-dispersive X-ray (EDX) spectra were measured by a JEOL JSM-6510A scanning electron microscope equipped with a JEOL JED 2300 EDX spectrometer. The concentration of metal ions was determined by a PerkinElmer ELAN DRC II inductively coupled plasma (ICP) mass spectrophotometer.

All of the adsorption experiments were carried out in batch mode. For a determination of the adsorption isotherm, CFP-g-PMHCTMA (5 mg) was placed in small plastic bottles containing 5 mL of the metal ion solution (10–280 $mg\ L^{-1}$) at

pH 3 and a temperature of 25 °C. The bottles were equilibrated on a thermostatic shaker. The adsorption amounts were calculated from the residual amounts of the metal ions in the solutions.

Kinetic experiments were conducted using 5 mg of CFP-g-PMHCTMA with 5 mL of 200 $mg\ L^{-1}$ aqueous solutions of metal ions. The samples were collected at different time intervals to determine the equilibrium point of adsorption.

The percent of metal adsorption in solution was evaluated using eq 7

$$\text{adsorption (\%)} = \frac{(c_i - c_e) \times 100}{c_i} \quad (7)$$

C_i ($mg\ L^{-1}$) = initial metal ion concentration; and C_e ($mg\ L^{-1}$) = equilibrated metal ion concentration.

The adsorption amounts were calculated from residual amounts of metal ions in solutions according to eq 8.

$$q_e = \frac{(C_i - C_e)V}{W} \quad (8)$$

where q_e ($mg\ g^{-1}$) is the adsorption capacity; V (L) is the volume of the metal solution, and W (g) is the mass of dry adsorbent.

5.3. Leaching of Metals from Waste Printed Circuit Board (WPCB) Using Aqua Regia. The metals in WPCBs were leached by aqua regia. In a typical procedure, WPCBs collected from waste computers were cut into 3×4 cm sizes. Then, 12 pieces of cut WPCBs were put into freshly prepared 30 mL portions of aqua regia and soaked for 30 min for complete leaching of metals into aqua regia. The resulting mixture was filtered, and the filtrate was analyzed by ICP-MS after proper dilution. The detected metal ions are V(V), Fe(III), Ni(II), Cu(II), Mn(II), Cr(III), Co(II), Zn(II), Pd(II), Au(III), and Ag(I), and the concentrations are indicated in Table S3.

■ ASSOCIATED CONTENT

Supporting Information

The Supporting Information is available free of charge at <https://pubs.acs.org/doi/10.1021/acsomega.1c06988>.

NMR data of the acylated MCHT ligand and additional figures and tables as described in the text (PDF) (PDF)

■ AUTHOR INFORMATION

Corresponding Author

Bungo Ochiai – Department of Chemistry and Chemical Engineering, Faculty of Engineering, Yamagata University, Yonezawa, Yamagata 992-8510, Japan; orcid.org/0000-0002-4376-8875; Phone: +81-238-26-3092; Email: ochiai@yz.yamagata-u.ac.jp

Author

M. K. Mohammad Ziaul Hyder – Department of Chemistry and Chemical Engineering, Faculty of Engineering, Yamagata University, Yonezawa, Yamagata 992-8510, Japan; Present Address: Department of Chemistry, Faculty of Engineering & Technology, Chittagong University of Engineering & Technology, Chattogram 4349, Bangladesh; orcid.org/0000-0002-6255-5349

Complete contact information is available at:

<https://pubs.acs.org/10.1021/acsomega.1c06988>

Notes

The authors declare no competing financial interest.

ACKNOWLEDGMENTS

The authors acknowledge a Japanese government scholarship to M.K.M.Z.H. from the Ministry of Education, Culture, Sports, Science and Technology of Japan to support this research at Yamagata University.

REFERENCES

- (1) Liu, Y.; Song, Q.; Zhang, L.; Xu, Z. Targeted Recovery of Ag-Pd Alloy from Polymetallic Electronic Waste Leaching Solution via Green Electrodeposition Technology and Its Mechanism. *Sep. Purif. Technol.* **2022**, *280*, 118944.
- (2) Barragan, J. A.; Alemán Castro, J. R.; Peregrina-Lucano, A. A.; Sánchez-Amaya, M.; Rivero, E. P.; Larios-Durán, E. R. Leaching of Metals from E-Waste: From Its Thermodynamic Analysis and Design to Its Implementation and Optimization. *ACS Omega* **2021**, *6* (18), 12063–12071.
- (3) Rao, M. D.; Singh, K. K.; Morrison, C. A.; Love, J. B. Challenges and Opportunities in the Recovery of Gold from Electronic Waste. *RSC Adv.* **2020**, *10* (8), 4300–4309.
- (4) Ding, Y.; Zhang, S.; Liu, B.; Zheng, H.; Chang, C.; Ekberg, C. Recovery of Precious Metals from Electronic Waste and Spent Catalysts: A Review. *Res. Conserv. Recycl.* **2019**, *141*, 284–298.
- (5) Xolo, L.; Moleko-Boyce, P.; Makelane, H.; Faleni, N.; Tshentu, Z. R. Status of Recovery of Strategic Metals from Spent Secondary Products. *Minerals* **2021**, *11* (7), 673.
- (6) Chancerel, P.; Meskers, C. E. M.; Hagelüken, C.; Rotter, V. S. Assessment of Precious Metal Flows During Preprocessing of Waste Electrical and Electronic Equipment. *J. Ind. Ecol.* **2009**, *13* (5), 791–810.
- (7) Wordsworth, J.; Khan, N.; Blackburn, J.; Camp, J. E.; Angelis-Dimakis, A. Technoeconomic Assessment of Organic Halide Based Gold Recovery from Waste Electronic and Electrical Equipment. *Resources* **2021**, *10* (2), 17.
- (8) Hagelüken, C.; Corti, C. W. Recycling of Gold from Electronics: Cost-Effective Use through Design for Recycling. *Gold Bull.* **2010**, *43* (3), 209–220.
- (9) Van Eygen, E.; De Meester, S.; Tran, H. P.; Dewulf, J. Resource Savings by Urban Mining: The Case of Desktop and Laptop Computers in Belgium. *Res. Conserv. Recycl.* **2016**, *107*, 53–64.
- (10) Park, Y. J.; Fray, D. J. Recovery of High Purity Precious Metals from Printed Circuit Boards. *J. Hazard. Mater.* **2009**, *164* (2–3), 1152–1158.
- (11) Gavrilescu, D.; Enache, A.; Ibănescu, D.; Teodosiu, C.; Fiore, S. Sustainability Assessment of Waste Electric and Electronic Equipment Management Systems: Development and Validation of the SUSTWEEE Methodology. *J. Cleaner Prod.* **2021**, *306*, 127214.
- (12) Ponghiran, W.; Charoensang, A.; Khaodhiar, S. The Environmental Impact Assessment of Gold Extraction Processes for Discarded Computer RAM: A Comparative Study of Two Leaching Chemicals. *J. Mater. Cycles Waste Manag.* **2021**, *23* (4), 1412–1422.
- (13) Oluokun, O. O.; Otunniyi, I. O. Kinetic Analysis of Cu and Zn Dissolution from Printed Circuit Board Physical Processing Dust under Oxidative Ammonia Leaching. *Hydrometallurgy* **2020**, *193*, 105320.
- (14) Gande, V. V.; Vats, S.; Bhatt, N.; Pushpavanam, S. Sequential Recovery of Metals from Waste Printed Circuit Boards Using a Zero-Discharge Hydrometallurgical Process. *Cleaner Eng. Technol.* **2021**, *4*, 100143.
- (15) Zhao, F.; Peydayesh, M.; Ying, Y.; Mezzenga, R.; Ping, J. Transition Metal Dichalcogenide–Silk Nanofibril Membrane for One-Step Water Purification and Precious Metal Recovery. *ACS Appl. Mater. Interfaces* **2020**, *12* (21), 24521–24530.
- (16) Mohebbi, A.; Abolghasemi Mahani, A.; Izadi, A. Ion Exchange Resin Technology in Recovery of Precious and Noble Metals. In *Applications of Ion Exchange Materials in Chemical and Food Industries*; Inamuddin, Rangreez, T. A., Asiri, A. M., Eds.; Springer International: 2019; pp 193–258. DOI: 10.1007/978-3-030-06085-5_9.
- (17) Ramesh, A.; Hasegawa, H.; Sugimoto, W.; Maki, T.; Ueda, K. Adsorption of Gold(III), Platinum(IV) and Palladium(II) onto Glycine Modified Crosslinked Chitosan Resin. *Biores. Technol.* **2008**, *99* (9), 3801–3809.
- (18) Pietrelli, L.; Ferro, S.; Vocciant, M. Eco-Friendly and Cost-Effective Strategies for Metals Recovery from Printed Circuit Boards. *Renew. Sustain. Energy Rev.* **2019**, *112*, 317–323.
- (19) Biswas, F. B.; Rahman, I. M. M.; Nakakubo, K.; Endo, M.; Nagai, K.; Mashio, A. S.; Taniguchi, T.; Nishimura, T.; Maeda, K.; Hasegawa, H. Highly Selective and Straightforward Recovery of Gold and Platinum from Acidic Waste Effluents Using Cellulose-Based Bio-Adsorbent. *J. Hazard. Mater.* **2021**, *410*, 124569.
- (20) Seidi, F.; Reza Saeb, M.; Huang, Y.; Akbari, A.; Xiao, H. Thiomers of Chitosan and Cellulose: Effective Biosorbents for Detection, Removal and Recovery of Metal Ions from Aqueous Medium. *Chem. Rec.* **2021**, *21* (7), 1876–1896.
- (21) Monier, M.; Akl, M. A.; Ali, W. M. Modification and Characterization of Cellulose Cotton Fibers for Fast Extraction of Some Precious Metal Ions. *Int. J. Biol. Macromol.* **2014**, *66*, 125–134.
- (22) Thakur, S.; Verma, A.; Kumar, V.; Jin Yang, X.; Krishnamurthy, S.; Coulon, F.; Thakur, V. K. Cellulosic Biomass-Based Sustainable Hydrogels for Wastewater Remediation: Chemistry and Prospective. *Fuel* **2022**, *309*, 122114.
- (23) O’Connell, D. W.; Birkinshaw, C.; O’Dwyer, T. F. Heavy Metal Adsorbents Prepared from the Modification of Cellulose: A Review. *Biores. Technol.* **2008**, *99* (15), 6709–6724.
- (24) Heinze, T.; Liebert, T. Unconventional Methods in Cellulose Functionalization. *Prog. Polym. Sci.* **2001**, *26* (9), 1689–1762.
- (25) Maaloul, N.; Oulego, P.; Rendueles, M.; Ghorbal, A.; Díaz, M. Enhanced Cu(II) Adsorption Using Sodium Trimetaphosphate-Modified Cellulose Beads: Equilibrium, Kinetics, Adsorption Mechanisms, and Reusability. *Environ. Sci. Pollut. Res.* **2021**, *28* (34), 46523–46539.
- (26) Luo, X.; Yuan, J.; Liu, Y.; Liu, C.; Zhu, X.; Dai, X.; Ma, Z.; Wang, F. Improved Solid-Phase Synthesis of Phosphorylated Cellulose Microsphere Adsorbents for Highly Effective Pb²⁺ Removal from Water: Batch and Fixed-Bed Column Performance and Adsorption Mechanism. *ACS Sustainable Chem. Eng.* **2017**, *5* (6), 5108–5117.
- (27) Yang, X.; Dong, Z.; Zhang, M.; Du, J.; Zhao, L. Selective Recovery of Ag(I) Using a Cellulose-Based Adsorbent in High Saline Solution. *J. Chem. Eng. Data* **2020**, *65* (4), 1919–1926.
- (28) Jafari, S.; Wilson, B.; Hakalahti, M.; Tammel, T.; Kontturi, E.; Lundström, M.; Sillanpää, M. Recovery of Gold from Chloride Solution by TEMPO-Oxidized Cellulose Nanofiber Adsorbent. *Sustainability* **2019**, *11* (5), 1406.
- (29) Kinemuchi, H.; Ochiai, B. Synthesis of Hydrophilic Sulfur-Containing Adsorbents for Noble Metals Having Thiocarbonyl Group Based on a Methacrylate Bearing Dithiocarbonate Moieties. *Adv. Mater. Sci. Eng.* **2018**, *2018*, 1–8.
- (30) Wang, Q.; Dang, Q.; Liu, C.; Wang, X.; Li, B.; Xu, Q.; Liu, H.; Ji, X.; Zhang, B.; Cha, D. Novel Amidinothiourea-Modified Chitosan Microparticles for Selective Removal of Hg(II) in Solution. *Carbohydr. Polym.* **2021**, *269*, 118273.
- (31) Patiño-Ruiz, D.; Bonfante, H.; De Ávila, G.; Herrera, A. Adsorption Kinetics, Isotherms and Desorption Studies of Mercury from Aqueous Solution at Different Temperatures on Magnetic Sodium Alginate-Thiourea Microbeads. *Environ. Nanotechnol. Monit. Manag.* **2019**, *12*, 100243.
- (32) Ueki, Y.; Seko, N. Synthesis of Fibrous Metal Adsorbent with a Piperazinyl-Dithiocarbamate Group by Radiation-Induced Grafting and Its Performance. *ACS Omega* **2020**, *5* (6), 2947–2956.
- (33) Xue, D.; Li, T.; Chen, G.; Liu, Y.; Zhang, D.; Guo, Q.; Guo, J.; Yang, Y.; Sun, J.; Su, B.; Sun, L.; Shao, B. Sequential Recovery of

Heavy and Noble Metals by Mussel-Inspired Polydopamine-Polyethyleneimine Conjugated Polyurethane Composite Bearing Dithiocarbamate Moieties. *Polymers* **2019**, *11* (7), 1125.

(34) Xiang, B.; Fan, W.; Yi, X.; Wang, Z.; Gao, F.; Li, Y.; Gu, H. Dithiocarbamate-Modified Starch Derivatives with High Heavy Metal Adsorption Performance. *Carbohydr. Polym.* **2016**, *136*, 30–37.

(35) Abu-El-Halawa, R.; Zabin, S. A. Removal Efficiency of Pb, Cd, Cu and Zn from Polluted Water Using Dithiocarbamate Ligands. *J. Taibah Univ.Sci.* **2017**, *11* (1), 57–65.

(36) Tan, Y. S.; Yeo, C. I.; Tiekink, E. R. T.; Heard, P. J. Dithiocarbamate Complexes of Platinum Group Metals: Structural Aspects and Applications. *Inorganics* **2021**, *9* (8), 60.

(37) Sun, Y.; Matsumura, Y.; Ochiai, B. Selective Ag⁺ Adsorption of Ureido Polymer Prepared by Cyclopolymerization Giving Large Ring Repeating Units. *ACS Appl. Polym. Mater.* **2020**, *2* (4), 1417–1421.

(38) Hyder, M. K. M. Z.; Ochiai, B. Selective Recovery of Au(III), Pd(II), and Ag(I) from Printed Circuit Boards Using Cellulose Filter Paper Grafted with Polymer Chains Bearing Thiocarbamate Moieties. *Microsys. Technol.* **2018**, *24* (1), 683–690.

(39) Ochiai, B.; Ogihara, T.; Mashiko, M.; Endo, T. Synthesis of Rare-Metal Absorbing Polymer by Three-Component Polyaddition through Combination of Chemo-Selective Nucleophilic and Radical Additions. *J. Am. Chem. Soc.* **2009**, *131* (5), 1636–1637.

(40) Joshi, G.; Rana, V.; Naithani, S.; Varshney, V. K.; Sharma, A.; Rawat, J. S. Chemical Modification of Waste Paper: An Optimization towards Hydroxypropyl Cellulose Synthesis. *Carbohydr. Polym.* **2019**, *223*, 115082.

(41) Adhikari, C. R.; Parajuli, D.; Inoue, K.; Ohto, K.; Kawakita, H.; Harada, H. Recovery of Precious Metals by Using Chemically Modified Waste Paper. *New J. Chem.* **2008**, *32* (9), 1634.

(42) Hyder, M. K. M. Z.; Ochiai, B. Synthesis of a Selective Scavenger for Ag(I), Pd(II), and Au(III) Based on Cellulose Filter Paper Grafted with Polymer Chains Bearing Thiocarbamate Moieties. *Chem. Lett.* **2017**, *46* (4), 492–494.

(43) Kihara, N.; Nakawaki, Y.; Endo, T. Preparation of 1,3-Oxathiolane-2-Thiones by the Reaction of Oxirane and Carbon Disulfide. *J. Org. Chem.* **1995**, *60* (2), 473–475.

(44) Pearson, R. G. Recent Advances in the Concept of Hard and Soft Acids and Bases. *J. Chem. Educ.* **1987**, *64* (7), 561–567.

(45) Losev, V.; Elsufeyev, E.; Borodina, E.; Buyko, O.; Maznyak, N.; Trofimchuk, A. Silicas Chemically Modified with Sulfur-Containing Groups for Separation and Preconcentration of Precious Metals Followed by Spectrometric Determination. *Minerals* **2021**, *11* (5), 481.

(46) Pan, X.-H.; Fu, L.-X.; Wang, H.; Xue, Y.; Zu, J.-H. Synthesis of Novel Sulfhydryl-Functionalized Chelating Adsorbent and Its Application for Selective Adsorption of Ag(I) under High Acid. *Sep. Purif. Technol.* **2021**, *271*, 118778.

(47) Kavakli, C.; Malci, S.; Tuncel, S. A.; Salih, B. Selective Adsorption and Recovery of Precious Metal Ions from Geological Samples by 1,5,9,13-Tetrathiacyclohexadecane-3,11-Diol Anchored Poly(p-CMS-DVB) Microbeads. *React. Funct. Polym.* **2006**, *66* (2), 275–285.

(48) Guibal, E.; Von Offenbergsweeney, N.; Vincent, T.; Tobin, J. M. Sulfur Derivatives of Chitosan for Palladium Sorption. *React. Funct. Polym.* **2002**, *50* (2), 149–163.

(49) Uheida, A.; Iglesias, M.; Fontàs, C.; Hidalgo, M.; Salvadó, V.; Zhang, Y.; Muhammed, M. Sorption of Palladium(II), Rhodium(III), and Platinum(IV) on Fe₃O₄ Nanoparticles. *J. Colloid Interface Sci.* **2006**, *301* (2), 402–408.

(50) Fan, L.; Luo, C.; Lv, Z.; Lu, F.; Qiu, H. Removal of Ag⁺ from Water Environment Using a Novel Magnetic Thiourea-Chitosan Imprinted Ag⁺. *J. Hazard. Mater.* **2011**, *194*, 193–201.

(51) Sharma, S.; Krishna Kumar, A. S.; Rajesh, N. A Perspective on Diverse Adsorbent Materials to Recover Precious Palladium and the Way Forward. *RSC Adv.* **2017**, *7* (82), 52133–52142.

(52) Sánchez, J. M.; Hidalgo, M.; Salvadó, V. Synthesised Phosphine Sulphide-Type Macroporous Polymers for the Preconcentration and

Separation of Gold (III) and Palladium (II) in a Column System. *React. Funct. Polym.* **2001**, *49* (3), 215–224.

(53) Parajuli, D.; Kawakita, H.; Inoue, K.; Funaoka, M. Recovery of Gold(III), Palladium(II), and Platinum(IV) by Aminated Lignin Derivatives. *Ind. Eng. Chem. Res.* **2006**, *45* (19), 6405–6412.

(54) Zhou, Y.; Hu, X.; Zhang, M.; Zhuo, X.; Niu, J. Preparation and Characterization of Modified Cellulose for Adsorption of Cd(II), Hg(II), and Acid Fuchsin from Aqueous Solutions. *Ind. Eng. Chem. Res.* **2013**, *52* (2), 876–884.

(55) Neris, J. B.; Luzardo, F. H. M.; da Silva, E. G. P.; Velasco, F. G. Evaluation of Adsorption Processes of Metal Ions in Multi-Element Aqueous Systems by Lignocellulosic Adsorbents Applying Different Isotherms: A Critical Review. *Chem. Eng. J.* **2019**, *357*, 404–420.

(56) Jadhav, U.; Hocheng, H. Hydrometallurgical Recovery of Metals from Large Printed Circuit Board Pieces. *Sci. Rep.* **2015**, *5* (1), 14574.